Geophys. J. Int. (1993) **115**, 829–838

Crustal wave propagation anomaly across the Pyrenean Range. Comparison between observations and numerical simulations

A. Chazalon,[1] M. Campillo,[1] R. Gibson[2] and E. Carreno[3]

[1]*Laboratoire de Géophysique Interne et Tectonophysique, Université Joseph Fourier, BP* 53 X, 38041 *Grenoble cedex, France*
[2]*Earth Resources Laboratory, MIT,* 42 *Carleton St, Cambridge, MA* 02142, *USA*
[3]*Servicio de Ingeniera Sismica, Instituto Geografico Nacional, Gral Ibanez, Ibero* 3, 28003 *Madrid, Spain*

Accepted 1993 April 23. Received 1993 March 31; in original form 1992 November 10

SUMMARY

Lg records analysis and numerical modelling of *Lg* propagation are used to find out to what extent this phase can be seen as a marker of unidentified structural anomalies in the crust. This study is based on *Lg* propagation through the Pyrenean range from earthquakes located in Spain.

We have first evaluated the mean value of the *S*-wave quality factor for central Spain. We have computed simultaneously the seismic station responses and the source functions. The correction for propagation effects, assuming a homogeneous attenuation and the theoretical calculation of the *Lg* excitation, lead to the seismic moment of each event. The moment magnitude obtained correlates well with the magnitude proposed by the local networks. This gives a confirmation of the *Q* model in the low-frequency range (1–5 Hz). As we intended to compare traces of different Spanish earthquakes recorded in France at different epicentral distances, we had to make amplitudes independent of propagation and source effects. Therefore, we corrected the spectral amplitudes for geometrical spreading, anelastic attenuation and normalized them to equal seismic moment.

We then plotted the records as a function of group velocity, in order to make up a fan profile along the Pyrenean axis. The resulting section reveals that in the central and the eastern parts of the range, neither the North Pyrenean Fault, nor the Moho jump deduced from seismic-refraction experiments and vertical seismics, seem to affect *Lg* propagation. However, there is an extinction of the *Lg* phase in the western part of the chain. The lateral extent of this area is correlated with a zone of positive gravity anomaly, probably linked to the presence of dense material of mantle origin. A numerical simulation in the low-frequency band indicates that the Moho topography inferred from deep seismic soundings does not explain the strength of the observed attenuation. Ray-tracing seismograms show that, at high frequency, the conclusion is the same. The attenuation effect due to lateral variation of structure should not be so strong. We, therefore, think that attenuation of guided waves is not due to large-scale geometry effects, but is due to local properties of the crustal materials, possibly apparent attenuation due to scattering on small-scale heterogeneities.

Key words: *Lg* waves, Pyrenees, quality factor, synthetic seismograms.

INTRODUCTION

In the range between 150 and several thousand kilometres, crustal waves are dominant on short-period seismograms in continental areas. Thus, the *Lg* phase, which consists of *S* waves trapped in the crust, is the major phase observed on regional records.

Lg amplitude is known to be sensitive to important changes in crustal structure: propagation paths through oceanic crust are the origin of high attenuation or extinction of the *Lg* phase, as found in the early analysis of this phase (Press & Ewing 1952; Båth 1954). Zones of strong local weakening of *Lg* also exist in continental domains. Such observations have been reported in the Himalayan Belt

(Ruzaikin *et al.* 1977), in the North Sea Graben (Kennett *et al.* 1985), in the Eurasian Shield (Baumgardt 1991) and in the south-western part of the Alpine range (Campillo *et al.* 1993).

It seems that some geological features partially or completely stop crustal guided wave propagation. Our purpose is to investigate what structure may produce these *Lg* amplitude variations and blockage effects. Is it a large-scale geometry result of a local attenuation or scattering effect? As there already exists evidence of an *Lg* propagation anomaly in the Western Alps, our study has been aimed at the analysis of *Lg* propagation across the Pyrenean range, in order to improve our knowledge about the influence of such orogenic structures.

DATA SPECIFICATIONS

For this study, we have used Spanish and French data obtained by the IGN (Instituto Geografico Nacional) array and the LDG (Laboratoire de Détection Géophysique) network respectively. All seismic stations are short-period vertical instruments with natural period of 1 s. The characteristics of the networks are described in an IGN report (IGN 1991) and by Nicolas *et al.* (1982) for the LDG network. We have examined records available from these two networks and we confirmed that *Lg* waves effectively propagate in France and in Spain, on both sides of the Pyrenean range. As we intended to study the propagation from natural sources located in Spain, to see whether or not *Lg* waves are able to cross the Pyrenees, we had to determine the anelastic attenuation of the crustal phases in Spain.

The data set consists of 12 earthquakes with hypocentres in the crust, recorded in Spain. Their parameters are described in Table 1. As is the case in most continental areas. *Lg* is the dominant phase on most of the records. The source–receiver pairs have been chosen in such a way that the propagation paths were sampling the central part of Spain, considered to be a stable continental area. We did not take into account stations located in southern Spain because we observed strong attenuation in the region of the Gaudalquivir sedimentary basin. Fig. 1 shows the paths used in this part of the study.

Table 1. The Spanish earthquakes looked at in this study (see Fig. 1).

Event	Date	Latitude °N	Longitude °W	H km	Ml LDG	Ml IGN	M_W-Lg
Ayamonte	20 12 89	23.286	-07.328	23.	5.4	5.0	4.4-4.8
Grandola	23 09 89	38.291	-08.655	18.	4.0		3.8-4.0
Cadix	25 10 87	36.361	-06.501	66.	4.8	4.2	3.6-4.0
Alicante	02 12 88	38.200	+00.315	20.	3.8	3.8	3.3-3.7
Sotos	07 11 87	43.000	-03.812	15.	3.9	3.8	3.5-3.7
Vilanova	10 08 86	41.128	-07.213	12.	4.0	4.3	3.6-3.9
Laza	30 08 89	42.105	-07.516	13.	3.7	3.9	3.5-3.7
Nazare	31 03 89	39.601	-09.493	25?	3.7	3.5	3.3-3.5
Camero	20 09 87	42.138	-02.476	05.	3.5	3.6	3.4-3.5
Aldea	24 05 88	38.400	-03.406	12.	3.8		3.4-3.7
Cucalon	06 07 87	40.951	-01.001	05.	3.5	3.3	3.1-3.3
Arnedo	29 11 88	42.146	-02.112	05.	3.1	3.2	2.9-3.1

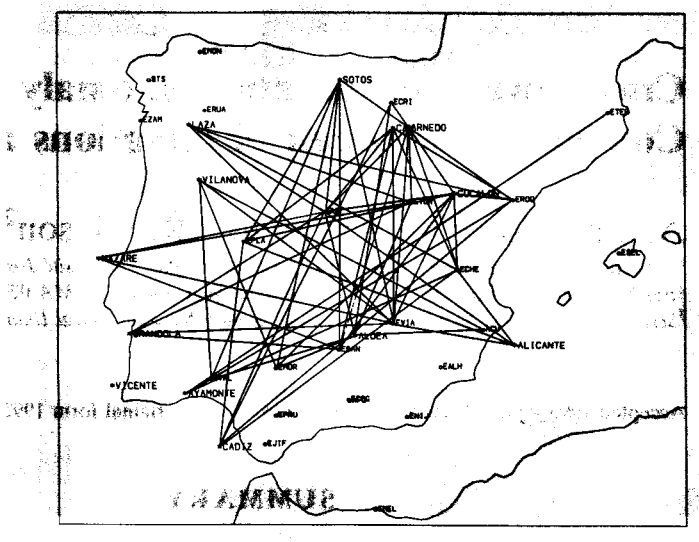

Figure 1. Locations of earthquake epicentres (stars) and IGN network stations (circles). On the map are also reported the paths used in the calculation of the mean value of crustal quality factor in Spain.

EVALUATION OF THE *S*-WAVE MEAN QUALITY FACTOR

To evaluate the *S*-wave mean quality factor, we used *Lg* phases that consist of multiply reflected *S* waves. Calculation of the crustal quality factor Q is done by computing the spectral density per time unit as a function of epicentral distance, in the time window providing the largest amplitudes, i.e. in the group velocity window 3.6–3.2 km s^{-1}.

For each station i and each earthquake j, this amplitude can be written in the form:

$$Aij(\mathrm{f}, \mathrm{d}) = Sj(\mathrm{f}) \cdot AA(\mathrm{f}, \mathrm{d}) \cdot E(\mathrm{d}) \cdot STi(\mathrm{f}), \quad (1)$$

f representing the frequency and d the epicentral distance. $Sj(\mathrm{f})$ is the source contribution, proportional to the seismic moment at low frequency. $AA(\mathrm{f}, \mathrm{d})$ is given by

$$\exp\left(\frac{-\pi \mathrm{f d}}{Q V_m}\right) \quad (2)$$

and represents the anelastic attenuation for a phase propagating with a mean velocity QV_m. $E(\mathrm{d})$ denotes the geometrical spreading in the time domain needed to correct the spectral density per time unit. It is taken in the form:

$$E(\mathrm{d}) = \mathrm{d}^{-0.83} \quad \text{(Campillo, Bouchon \& Massinon 1984)} \quad (3)$$

$STi(\mathrm{f})$ is the station response, corresponding to the effects of local geology structure.

This equation is solved by an iterative process given in detail by Campillo, Plantet & Bouchon (1985). Only the data obtained for earthquakes that were recorded by at least four stations, were used. We first took $ST = 1$ and evaluated the mean value of Q by least-square fitting for each earthquake. We then computed the mean value of Q for the entire set of events. ST could be evaluated by computing a simple residue at each station. This process converged after a few iterations. The root-mean-square residue between the

observed amplitudes and the ones predicted by eq. 1 was computed to check the convergence and the stability. The shape of the displacement spectrum was obtained after deconvolution of the instrumental response of the IGN network stations. Thus, we got the source-displacement spectra in m s.

We found $Q(f)$ in the form:

$$Q = (330 \pm 30) f^{0.51 \pm 0.06} \quad (4)$$

This result is close to the mean crustal quality factor computed for central France (Campillo *et al.* 1985).

ESTIMATION OF THE SEISMIC MOMENTS

We computed the seismic moment using the theoretical excitation of *Lg* for a point source dislocation. We neglected the radiation pattern since *Lg* is a superposition of *S* waves leaving the source in a wide range of take-off angles. To perform the estimation, we computed synthetic seismograms in a flat layered medium corresponding to the crustal structure of central Spain. Table 2 summarizes the characteristics of the model.

The theoretical calculation was performed, for a seismic moment of 1, using the discrete wavenumber representation (Bouchon 1981), combined with the Kennett propagation technique (1983). We evaluated the *Lg* spectral density from the synthetics in exactly the same way as for the data. We can, therefore, obtain the theoretical value of the term *S* of eq. 1 for a unit moment. For frequencies lower than the corner frequency, we can relate the seismic moment to the observed amplitudes, corrected for spreading and attenuation. To test the accuracy of our results we have calculated the *Lg* magnitudes from each seismic moment value, from which we deduced M_w as defined by Kanamori (1977) M_w is given by:

$$\log M_0 = 1.5 M_w + 9 \quad (M_0 \text{ in Nm}). \quad (4)$$

Table 1 presents the local magnitudes reported in the bulletins and the values of our M_w magnitudes. We can see that the seismic moments measured from the *Lg* phase vary consistently with the magnitudes proposed by the local networks. Fig. 2 shows the source spectra which allow us to find out the seismic moments and the magnitude values. We plotted all spectra on a log–log diagram, in order to compare their shape and their dimension. One can see that the corner frequency measured on our spectra varies between 3 and 8 Hz. Considering the events with seismic moment between 10^{13} and 10^{16} Nm i.e. $M_w < 5$, and assuming a self-similar model, f_c should be in the range 0.6–7 Hz for a 100 to 200 bars stress drop. Beyond f_c, the observed high-frequency spectra decrease as ω^{-2}.

Table 2. Crustal model used for the numerical calculations.

Layer Thickness (km)	P-Wave Velocity (km/sec)	S-Wave Velocity (km/sec)	Density (g/cm3)	P-Wave Q	S-Wave Q
2	3.3	2.5	2.1	10000	10000
5	6.1	3.48	2.8	10000	10000
4	5.6	3.18	2.7	10000	10000
13	6.4	3.58	2.9	10000	10000
7	6.85	3.90	3.0	10000	10000
	8.05	4.45	3.3	10000	10000

The *Lg* magnitudes we found are systematically smaller than those given by the local networks from direct waves. We have tested that the crustal model used for the numerical simulation of *Lg* propagation has no significant influence on the seismic moment values. On the other hand, changes in the parameters of fault geometry cause variations in the *Lg* magnitudes. However, azimuthal dependence is weaker for *Lg* than for direct waves (Campillo 1990) because this phase is made up of a superposition of rays, sampling a wide range of take-off angles. The good agreement of the linear correlation we obtained between *Lg* moment magnitudes and local magnitudes confirms the possibility of using the source spectra to correct the amplitudes.

PROPAGATION ANALYSIS THROUGH THE PYRENEES

Most of the earthquakes whose records were used for the Q calculation did not provide data of adequate quality at the French stations because of the great epicentral distances. Only four events located in northern Spain provide a large enough signal-to-noise ratio: Sotos, Cucalon and the two closely spaced events Camero and Arnedo (see Fig. 1).

First we looked at the records obtained at the French station EPF, which is located in the Pyrenees, north of the North Pyrenean Fault (NPF, Fig. 3). This zone of deep subvertical faults is a major structural feature of the mountain range, clearly apparent in the oriental and in the central Pyrenees. In the western Pyreness, it is assumed that the discontinuity is overlain by Cretaceous sediments. The NPF constitutes the limit of the North Pyrenean Zone and the axial zone of the range. The available information concerning the tectonics of the region shows that, in the central part of the range (Fig. 4), an underthrust of the Iberic crust to the North takes place along the NPF (Pinet *et al.* 1987; Choukroune *et al.* 1989). On the other hand, the oceanic lithosphere in the Gulf of Biscay dives under the Iberic plate (Boillot *et al.* 1971).

For the earthquakes we examined, the seismograms recorded at EPF have the same typical shape of continental short-period records as observed at all nearby Spanish stations: the crustal wave *Pg* and *Lg* are dominant. This is illustrated in Fig. 5 (a and b): the *Lg* phase produces a clear onset at 3.5 km s^{-1}. However, the records obtained at stations in central France show very different characteristics. The corresponding paths are plotted in Fig. 6. In the case where the path crosses the western part of the Pyrenean Chain, the larger arrivals on the seismograms have a group velocity higher than *Lg* (about 4.2 km s^{-1}) and consist of the mantle wave *Sn* (Fig. 5c). The *Lg* phase vanishes along this path. For a path that crosses the central part of the chain, *Sn* and *Lg* exhibit similar amplitudes (Fig. 5d). These seismograms suggest that the regional phases are affected very differently when they cross the Pyrenees at different locations along the axis of the range.

In order to verify this effect we plotted a series of seismograms as a function of the location where the waves cross the Pyrenees. We measured the locations of the crossing along an axis from Bilbao to Perpignan shown as a

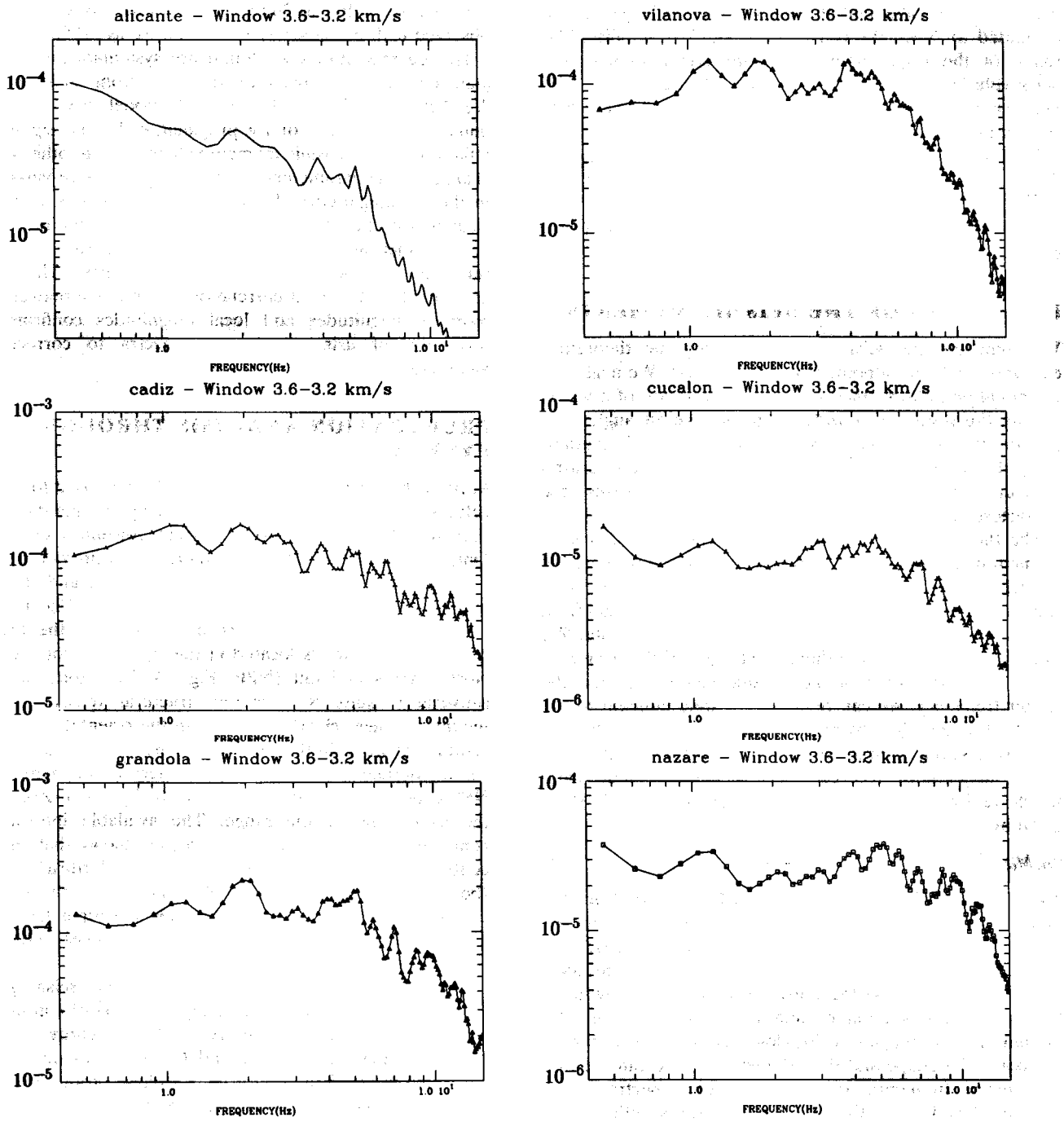

Figure 2. Source-displacement spectra plotted for each earthquake in m s.

thick solid line in Fig. 6. The identification of the various regional phases in the data set is simplified by plotting the records as a function of group velocity. We consider the records in France from a series of earthquakes in northern Spain (Table 3 and Fig. 6). The records are bandpassed between 1 and 5 Hz. Amplitudes are corrected for geometrical spreading, anelastic attenuation and normalized to equal seismic moment. The effect of attenuation is crudely removed from the whole seismogram by correcting the spectra with a filter defined from our results of the quality factor for *S* waves (eq. 4). The seismic moment used for the normalization is obtained from the least-square regression of the spectral amplitude of *Lg* with distance for the LDG stations. In case of a strong effect of attenuation of *Lg* at the crossing of the Pyrenees, the moment is underestimated. This results in an unrealistically high amplitude of the other seismic phases such as *Sn*.

Figure 7 presents the section obtained from these Spanish earthquakes recorded in France. One can see that the sampling is not homogeneous because of the poor distribution of earthquakes in northern Spain correctly recorded in France. However, we notice that the waveform is very different in the east and in the west side of the Pyrenean range. In the east, the maximum amplitudes

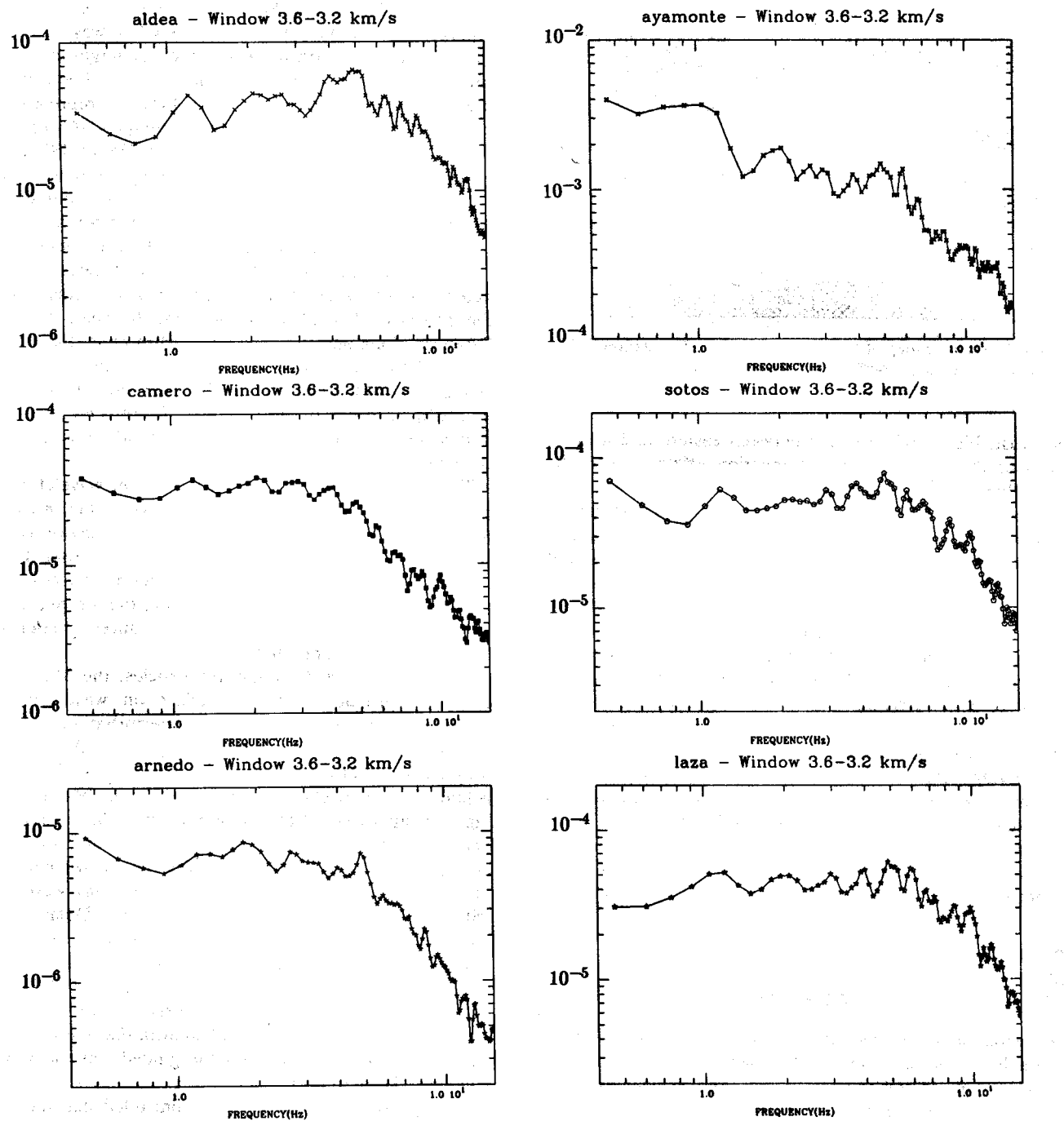

Figure 2. (*Continued.*)

appear for group velocities between 3.5 and 3.0 km s^{-1}: these waves are clearly *Lg* phases. In the west, the largest amplitudes are seen between 4.5 and 4.0 km s^{-1}. These phases are *Sn* waves corresponding to upper mantle propagation.

As has already been noticed, the way we perform the normalization of seismic moment can explain why the amplitudes of *Pn* and *Sn* waves in the western part appear much higher than those in the eastern part. Another reason is the way we corrected amplitudes with distance. The amplitude corrections for spatial attenuation are strictly valid only in the group velocity window 3.2–3.6 km s^{-1}, i.e. for the *Lg* wave. Phases for which group velocity is greater than the *Lg* wave velocity are all the more amplified since epicentral distance and frequency increase. Even if the amplitude values are not exact along the entire record, this figure illustrates the *Lg* blockage and the relative *Sn*-wave amplification in the western Pyrenees. The *Sn* waves cannot be observed in the eastern Pyrenees because their amplitudes are much smaller than the ones of *Pg* and *Lg*. If we accept that *Sn* is not sensitive to crustal structure and that the mantle is almost homogeneous beneath this region, the variation of the ratio of amplitude *Sn* to *Lg* at a given distance is a crude measure of the variation of attenuation in

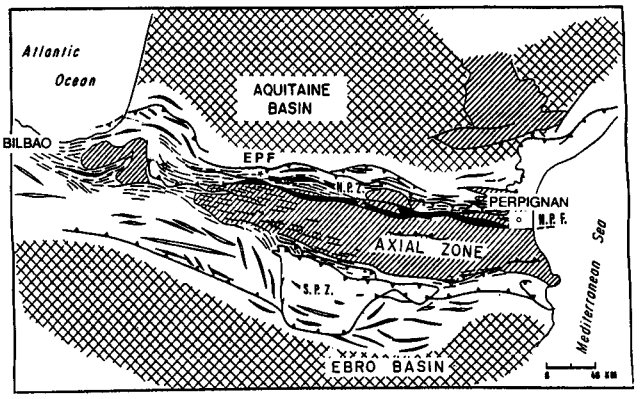

Figure 3. Tectonic map of the Pyrenean region. The station EPF is reported on the figure. NPF: North Pyrenean Fault.

the crust. Fig. 7 indicates that between eastern and western parts of the Pyrenees, the attenuation effect changes by more than one order of magnitude.

However, for all these earthquakes, the *Lg* phase can be observed at EPF station. The presence of the *Lg* phase in the east and at EPF indicates that the *Lg* blockage is not simply associated with the NPF, which lies along the entire eastern and central part of the range. On the other hand, the *Lg* phase vanishes when it crosses the western part of the mountain chain and the energy seems to propagate mostly as the *Sn* wave. This anomaly seems to have a lateral extent of about 100 km. It is noteworthy that this zone of attenuation corresponds to a zone of strong positive gravity anomaly called the 'Labourd anomaly', whose origin is not definitively known. The areas with positive Bouguer anomaly are shown in grey in Fig. 6. A similar anomaly of propagation of the crustal phase *Lg* has been reported in the Western Alps (Campillo *et al.* 1993), correlated with a positive Bouguer anomaly. Crustal materials of deep origin might be associated with both features.

NUMERICAL SIMULATIONS IN MULTILAYERED MEDIA WITH IRREGULAR INTERFACES

We attempted to understand why *Lg* is not observed through the western part of the range. To investigate the influence of crustal geometry on *Lg* propagation, we performed some numerical modelling in laterally heterogeneous models for the *SH* case. Since *Lg* consists of a superposition of post-critically reflected *S* waves, the *SH* case must present most of the effect of the large-scale lateral variations of Moho depth. The calculation method combines the discrete wavenumber Green's function representation with boundary-integral equation techniques (Campillo & Bouchon 1985; Bouchon, Campillo & Gaffet 1989). The wavefield produced by the interfaces is considered to be equivalent to the radiation of body forces distributed along the boundaries. The inversion of a propagator matrix was performed for each interface, so that the computation time and the memory required varies only linearly with the number of interfaces. As many seismic experiments revealed the presence of a 10 km Moho jump between the North Pyrenean Zone and the axial zone (Hirn *et al.* 1980; Roure *et al.* 1989), we have first designed a model with simple change in crustal thickness (Fig. 8a), the Moho being deeper on the Spanish side of the Pyrenees. There is no attenuation in this model: only the topography of the Moho is taken into account.

The synthetic seismograms, with a Ricker wavelet of 1.5 s period as the source function, are shown in Fig. 8(b). The maximum frequency reached is 1 Hz. The reduction velocity is 3.5 km s^{-1}, which is the *S*-wave velocity chosen for the crust. One can see the successive reflection branches, which consistute the reflected energy forming the *Lg* phase. The *Sn* head-wave branch appears for distances greater than 250 km with small amplitudes.

We can check that, at low frequencies, the Moho jump does not produce a notable effect on waveforms and amplitudes. One can notice a weak perturbation above the Moho jump, but amplitudes are as large beyond the jump as they are ahead of it. The use of boundary integral equations is limited to relatively low frequencies simply because of the high computation time required by this quasi-exact approach. In order to check the validity of our conclusions at higher frequency, we used the ray theory to compute an 'infinite frequency' response. The calculations were made with the same model of Moho topography. Details of the computations with the paraxial ray approach and of the comparison with the boundary-integration equation method results are given in Gibson & Campillo (1993). The synthetics obtained (Fig. 8c) are very similar to those of boundary integral equations and confirm that the Moho step will only have weak effect on the guided wave amplitude, whatever the frequency band is.

From these numerical tests we concluded that the Moho

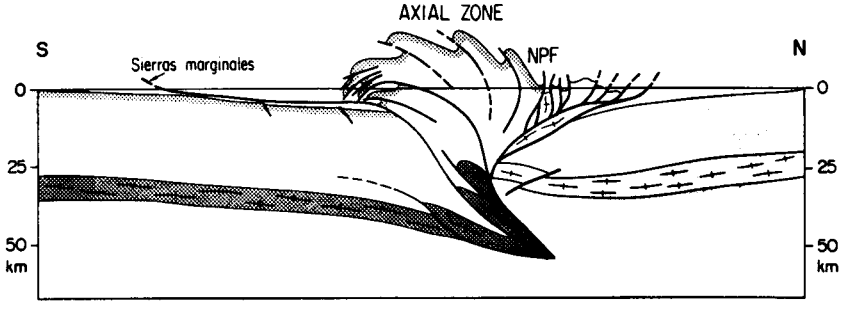

Figure 4. Cross-section showing the crustal geometry and the Moho topography from the Ebro basin in the south to the Aquitaine basin in the north, in the central part of the mountain range (from Roure *et al.* 1989).

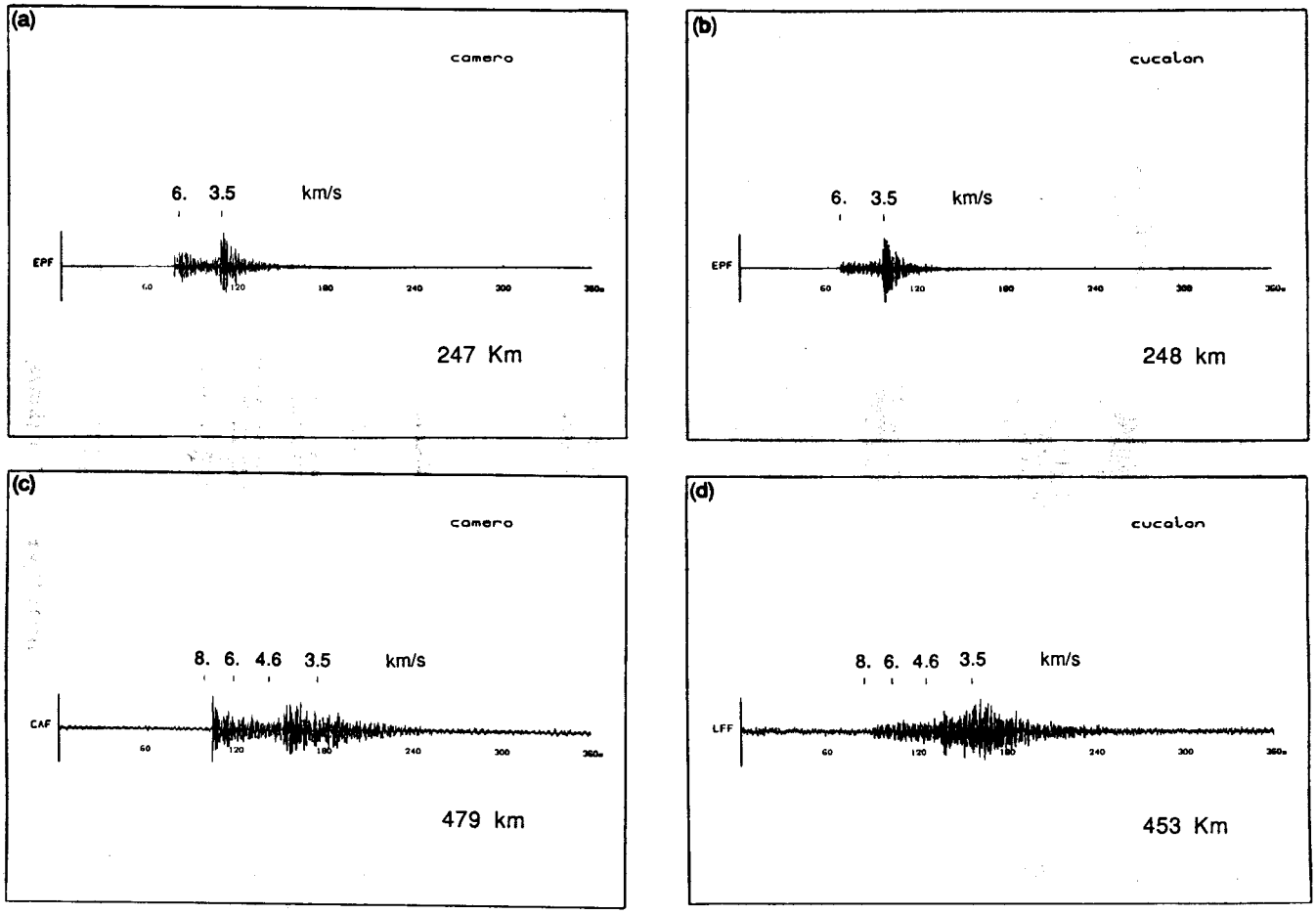

Figure 5. Short-period records obtained for earthquakes 'Camero' and 'Cucalon' at station EPF (a and b) and in central France (c and d). The corresponding paths are plotted in Fig. 6. The group velocity is indicated in order to make easier the identification of the different phases.

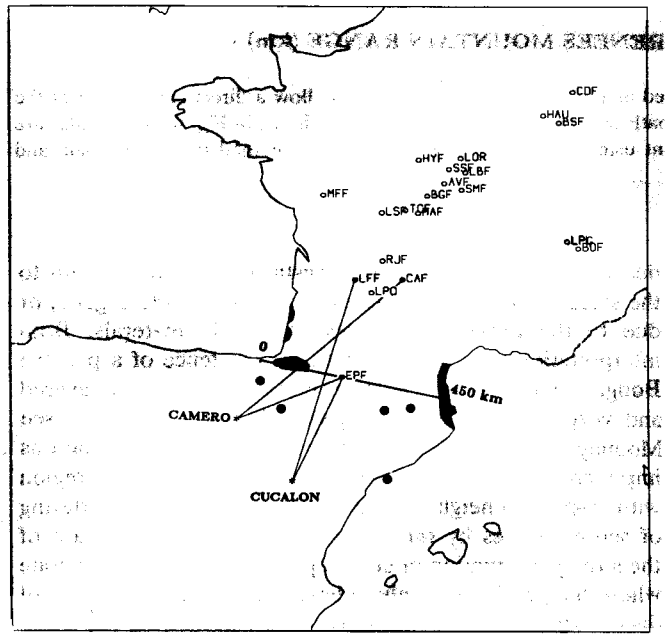

Figure 6. Map showing the location of earthquakes in Spain (block dots) and the seismic stations in France (circles) used to study regional phases crossing the Pyrenees. The lines correspond to the path of the seismograms shown in Fig. 5. The heavy line indicates the axis used to locate the crossing of the chain for the different paths. The grey zones indicate a positive Bouguer gravity anomaly.

jump cannot be the reason for the vanishing *Lg* wave. This is strongly supported by the observation that *Lg* waves are not attenuated in the Eastern Pyrenees. We must, therefore, examine in more detail the influence of the particular structure of the western part of the chain.

Figure 9(a) describes the second model, which includes results of recent deep seismic investigations conducted in the western Pyrenees (preliminary interpretation of the structure of the lithosphere along the Pyrenees–Arzacq Ecors profile, M. Daignières, private communication). These experiments suggest a zone of anomalously high

Table 3. Earthquakes in northern Spain.

Date	Time	Latitude °N	Longitude °W	MI LDG
07 04 86	23h32'07	42.91	-1.90	3.1
27 10 86	06h48'12	39.88	-1.12	3.5
24 08 87	18h43'06	41.01	1.49	4.4
20 02 88	16h38'48	42.40	1.48	3.8
16 03 88	21h19'02	42.38	2.17	3.8
26 07 90	16h29'32	42.37	-1.29	3.7
20 08 90	12h22'33	40.26	-0.92	3.4

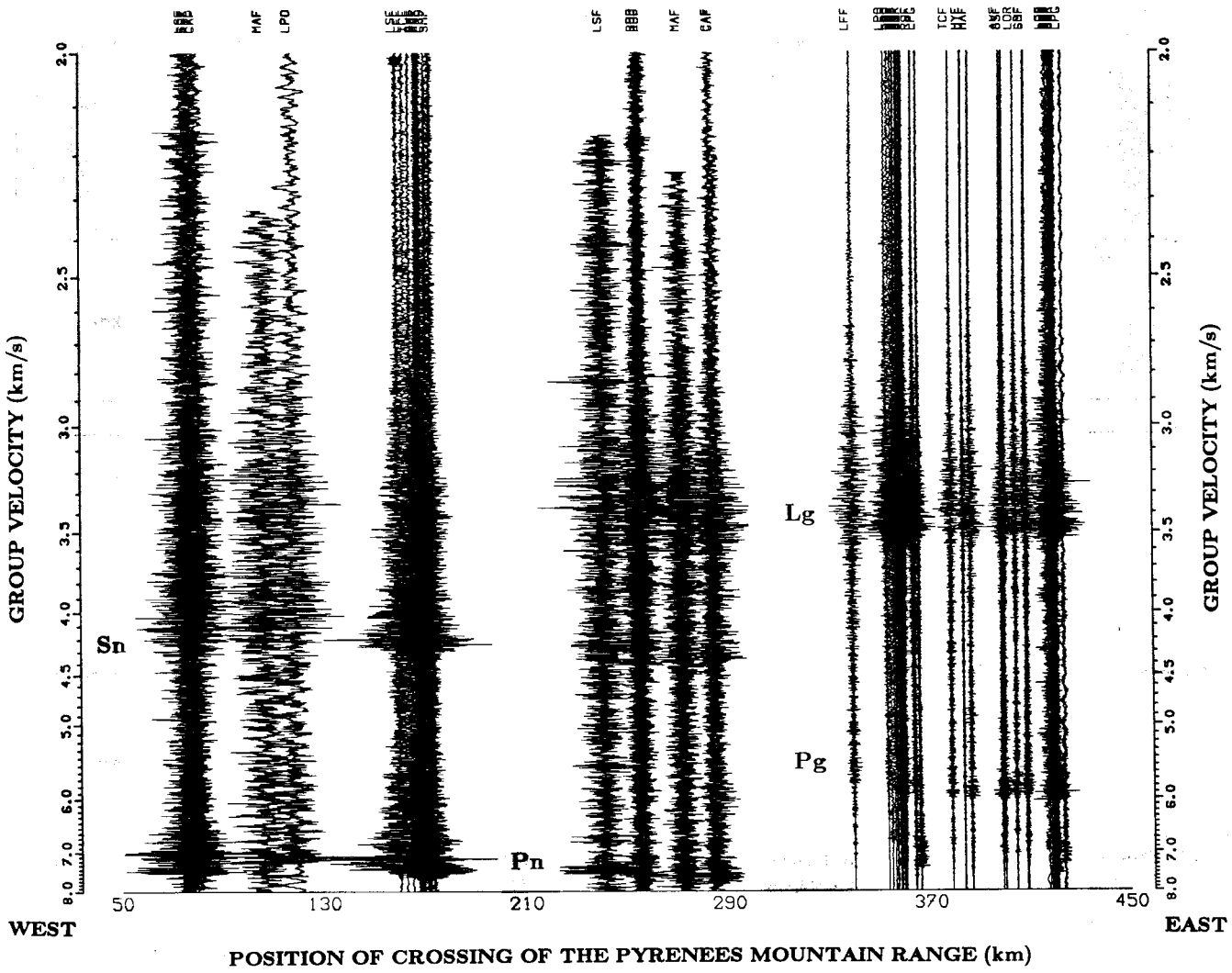

Figure 7. Seismograms obtained in France for earthquakes in Spain plotted as function of group velocity to allow a direct comparison of the traces. The horizontal axis represents the position of the crossing of each path with the line Bilbao–Perpignan shown in Fig. 6. Amplitudes are corrected for propagation effects and normalized to equal seismic moment using the propagation parameters obtained in central Spain and central France.

velocity in the crust, in addition to the Moho jump. We, therefore, investigated the influence of such a structure.

The synthetic seismograms from this second model are shown in Fig. 9(b). One can notice that the *Sn* wave is stronger than in the previous model. Therefore, as observed on the real data, the *Sn*/*Lg* amplitude ratio is higher for the rays travelling through such a zone. But the *Lg* wave is not much affected: the amplitude of the *Lg* wave train is still large beyond the velocity anomaly area. Therefore, the geometry of this structure can not account for the almost complete extinction of the *Lg* phase observed on the data.

This energy blockage must then be explained by the local properties of the crustal material rather than by the large-scale geometry of the crust–mantle structure. The theoretical result is in a good agreement with the observation that *Lg* can propagate across the eastern part of the mountain range where the jump of the Moho between north and south is present as in the western part. The high velocities observed in this area where *Lg* disappears may be due to the presence of lower crustal blocks, brought up to the surface during the compression phases of the orgeny, or due to the presence of slices of mantle materals. Both interpretations would agree with the existence of a positive Bouguer anomaly. As the lower crust is known to be layered and very reflective in many parts of western Europe (see Mooney & Brocher 1987, for a review), both interpretations imply an increased heterogeneity of the crust in this region with respect to neighbouring areas. An enhanced scattering of seismic waves by this heterogeneity may be the case of the strong attenuation of crustal phases observed in the zone where the gravity anomaly indicates intrusion of material of deep origin into the upper crust.

CONCLUSION

We combined observations and numerical simulations in order to study crustal wave propagation through the Pyrenees. We first computed a mean crustal value of the

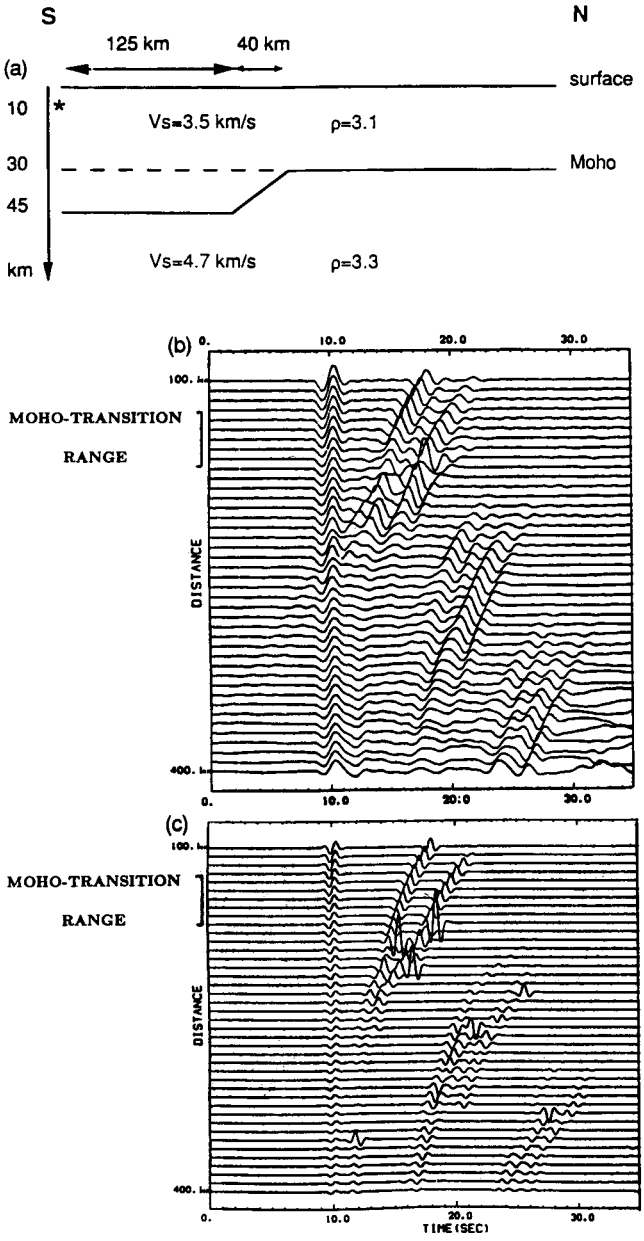

Figure 8. Influence of the Moho topography on *Lg* propagation: (a) model used with a simple variation of the Moho depth; (b) synthetic seismograms obtained using the boundary integral equation method; (c) synthetic seismograms obtained using the asymptotic ray theory. All synthetics are plotted using a reduction velocity of 3.5 km s^{-1}.

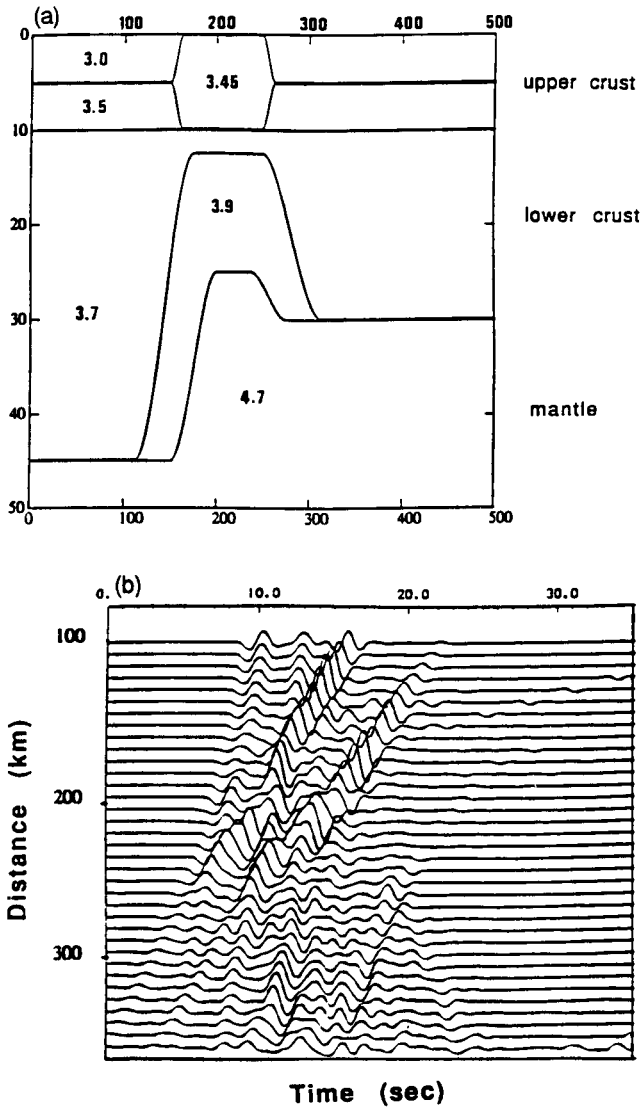

Figure 9. Influence of the Moho topography on *Lg* propagation: (a) model used with a Moho jump and introduction of high-velocity bodies in the crust; (b) synthetic seismograms obtained using the boundary integral equation method. Synthetics are plotted using a reduction velocity of 3.5 km s^{-1}.

S-wave quality factor for central Spain to evaluate intrinsic attenuation along the paths. Q has been found in the form

$$Q = 330f^{0.51}.$$

The seismogram analysis shows that in the central and eastern part of the mountain chain the North Pyrenean Fault does not block *Lg* propagation and that the Moho jump found in this region does not block either. In spite of the fact that the jump of the Moho is present all along the mountain range, a localized zone of attenuation exists in the western part of the Pyrenees, correlated with a positive Bouguer anomaly. As similar observations were made in the Alps in the Ivrea region and as numerical modellings show that geometrical effects do not explain the observed extinction of *Lg* waves, it seems that the general conclusion can be drawn that strong attenuation of guided waves is probably due to local crustal properties. Scattering by small-scale heterogeneities, such as lower crust or mantle slices, may be the cause of strong attenuation in the frequency range considered here. This interpretation is coherent with the observation of high seismic velocity and the position of a Bouguer anomaly in these regions.

ACKNOWLEDGMENTS

We thank J. L. Plantet and Y. Cansi (LDG, CEA) and the technical staffs of the LDG and IGN networks for their help in making available the records needed for this study. G. Müller and two anonymous reviewers made valuable

suggestions to improve this work. This work was partially supported by the project 'A.A. Tomographie' of INSU/CNRS (France) and by DARPA (USA) under contract 80-0082.

REFERENCES

Båth, M., 1954. The elastic waves *Rg* and *Lg* along Eurasiatic paths, *Arkiv Geofysic*, **2**, 295–342.

Baumgardt, D. R., 1991. High frequency array studies of long range *Lg* propagation and the causes of *Lg* blockage and attenuation in the Eurasian continental craton, *Final Report PL-TR-91-2059(II)*, Phillips Laboratory.

Boillot, G., Dupeuble, P. A., Lamboy, M., D'Ozouville, L. & Sibuet, J. C., 1971. Une hypothèse d'évolution tectonique du golfe de Gascogne, in *Histoire structurale du golfe de Gascogne*, pp. V.6–1—V.6–52, eds Debyser, J., Lepichon, X. & Montadert, L., Technip, Paris.

Bouchon, M., 1981. A simple method to calculate Green's function for elastic layered media, *Bull. seism. Soc. Am.*, **71**, 959–971.

Bouchon, M., Campillo, M. & Gaffet, S., 1989. A boundary integral equation—discrete wavenumber representation method to study wave propagation in multilayered media having irregular interfaces, *Geophysics*, **54**, 1134–1140.

Campillo, M., 1990. Propagation and attenuation characteristics of the crustal phase *Lg*, *Pure appl. Geophys.*, **132**, 1–19.

Campillo, M. & Bouchon, M., 1985. Synthetic *SH* seismograms in a laterally varying medium by the discrete wavenumber method, *Geophys. J. R. astr. Soc.*, **83**, 307–317.

Campillo, M., Bouchon, M. & Massinon, B., 1984. Theoretical study of the excitation, spectral characteristics and geometrical attenuation of regional seismic phases, *Bull. seism. Soc. Am.*, **74**, 79–90.

Campillo, M., Plantet, J. L. & Bouchon, M., 1985. Frequency dependent attentuation in the crust beneath Central France from *Lg* waves, data analysis and numerical modeling, *Bull. seism. Soc. Am.* **75**, 1395–1411.

Campillo, M., Feignier, B., Bouchon, M. & Bethoux, N., 1993. Attenuation of crustal waves across the Alpine range, *J. geophys. Res.*, **98**, 1987–1996.

Choukroune, P. & ECORS Team, 1989. The ECORS Pyrenean deep seismic profile: reflection data on the overall structure of an orogenic belt, *Tectonics*, **8**, 23–39.

Gibson, R. & Campillo, M., 1993. Numerical simulation of high- and low-frequency *Lg*-wave propagation, *Geophys. J. Int.*, submitted.

Hirn, A., Daigneres, M., Gallart, J. & Vadell, M., 1980. Explosion seismic sounding of throws and dips in the continental Moho, *Geophys. Res. Lett.* **7**, 263–266.

Instituto Geografico Nacional, 1991. Spanish National Seismic Network, in *Seismicity, Seismotectonics and Seismic Risk of the Ibero–Maghrebian Region*, pp. 3–16, eds Mezcua, J. & Udias, A., Monografia No. 8 IGN, Madrid.

Kanamori, H., 1977. The energy release in great earthquakes, *J. geophys. Res.*, **82**, 2981–2987.

Kennett, B. L. N., 1983. *Seismic wave propagation in stratified media*, Cambridge University Press, Cambridge.

Kennett, B. L. N., Gregersen, S., Mykkelveit, S. & Newmark, R., 1985. Mapping of crustal heterogeneity in the North Sea Basin via the propagation of *Lg* waves, *Geophys. J. R. astr. Soc.*, **83**, 299–306.

Mooney, W. D. & Brocher, T. M., 1987. Coincident seismic reflection/refraction studies of the continental lithosphere: a global review, *Rev. Geophys.*, **25**, 723–742.

Nicolas, M., Massinon, B., Mechler, P. & Bouchon, M., 1982. Attenuation of regional phases in Western Europe, *Bull. seism. Soc. Am.*, **72**, 2089–2106.

Pinet, B., Montadert, L., Curnelle, R., *et al.*, 1987. Crustal thinning on the Aquitaine shelf, Bay of Biscay, from deep seismic data, *Nature*, **325**, 513–516.

Press, F. & Ewing, M., 1952. Two slow surface waves across North America, *Bull. seism. Soc. Am.*, **42**, 219–228.

Roure, F., Choukroune, P., Berastegui, X., Munoz, J. A., Villien, A., Matheron, P., Bareyt, M., Seguret, M., Camara, P. & Deramond, J., 1989. ECORS deep seismic data and balanced cross-sections: geometric constraints on the evolution of the Pyrenees, *Tectonics*. **8**, 41–50.

Ruzaikin, A. I., Nersesov, I. L., Khalturin, V. I. & Molnar, P., 1977. Propagation of *Lg* and lateral variations in crustal structure in Asia, *J. geophys. Res.*, **82**, 307–316.